



Synthesis of syntactic steel foam using mechanical pressure infiltration

G. Castro*, S.R. Nutt

1. Department of Chemical Engineering and Materials Science, University of Southern California, Los Angeles, CA 90089-0241, USA

* Corresponding author at: 15654 E.Grovecenter St., Covina, CA 91722, USA. Tel.: +1 626 388 7858; fax: +1 213 740 7797. E-mail address: gerhardc@usc.edu (G. Castro)

Abstract: Steel foam offers potential advantages over aluminum foams and other metallic foams. The inherent strength of steel combined with the reduced density of foam presents an attractive material with greater strength and modulus than light alloy foams, greatly reduced density relative to solid steel, and efficient energy absorption. However, thus far there have been few reports describing efforts to produce steel foam, and these have relied on powder metallurgical approaches as opposed to molten state processing.

This study demonstrates a feasible synthesis method to consistently produce lab-scale foam samples with uniform distributions of microspheres and negligible unintended porosity using a simple liquid state method of infiltration. To accomplish this, the effects of process parameters were investigated. The preheat temperature of the microspheres must be close to the melting temperature of steel and a minimum pressure must be exerted to produce the steel infiltration into the microspheres. Syntactic foams with relative density of 0.54 were achieved. The resultant syntactic foams were characterized by chemical analysis, microstructural analysis and hardness measurement. The basic mechanical properties of two different steel compositions were studied under compression loading,

Please cite this article as Castro and S. Nutt , “**Synthesis of syntactic steel foam using mechanical pressure infiltration**” Mater Sci & Engrg A 535 (2012) 274-280 DOI<<http://dx.doi.org/10.1016/j.msea.2011.12.084>>



one with a ferrite microstructure and the other with a pearlite microstructure. The pearlite foam has greater compression strength and energy absorption capacity than the ferrite foam. The properties of the steel syntactic foams were compared to those of steel foams reported elsewhere. Prospects and challenges for achieving higher energy absorption capacity are discussed.

Key words: Steel, Ceramic microspheres, Pressure infiltration, Compression

1. Introduction

Prior efforts to produce steel foams have involved the use of powder metallurgy techniques [1] and [2]. One such technique involved the use of hollow ceramic/metallic microspheres to produce syntactic foams. Interstitial spaces between close-packed microspheres were filled with steel powder, and the mixture was subsequently sintered to produce the final syntactic foam [2]. A second approach involved the use of granular carbonate compounds as foaming agents, which were blended and compacted with steel powder, then melted to expand the foam (stochastic foams) [1]. Although the powder metallurgical approach is convenient and affords process control, liquid state methods afford some advantages, particularly because casting is generally a less expensive route to transform raw materials into usable components [3].

Producing foams from molten steel presents processing challenges, primarily because of the high temperatures involved. Despite these challenges, attempts have been made to produce steel foams from molten steel via the Gasar process [4], which is based on the nucleation of gas during solidification of a supersaturated steel melt. Syntactic steel foams represent a new class of metal foams. There have been only a few reports describing this approach because the procedures

Please cite this article as Castro and S. Nutt , “**Synthesis of syntactic steel foam using mechanical pressure infiltration**” Mater Sci & Engrg A 535 (2012) 274-280 DOI<<http://dx.doi.org/10.1016/j.msea.2011.12.084>>



commonly employed to produce aluminum and magnesium syntactic foams (e.g. vacuum, gas pressure, centrifugal force, stir casting technique, etc.) cannot be readily used to process ferrous alloys. Steel matrix composites (steel and alumina) have been produced by pressureless infiltration using titanium as an activator for the infiltration [5] and [6], thus avoiding the need for external force to achieve infiltration.

The proposed method of producing syntactic steel foam is based on simple mechanical pressure infiltration – no vacuum, gas pressure, centrifugal force or stir casting methods are involved – and the method requires only low-cost materials (low-carbon steel and alumina microspheres). Hollow alumina microspheres are used because of the inherent resistance to high temperatures (molten steel) and high strength. A customized induction furnace for melting small amounts of steel (less than one kilogram) was designed and built for this purpose. One of the limitations of using an induction furnace for melting steel (as opposed to a resistance furnace) is that the temperature of the melt is not easily measured, either intermittently or continuously. Using a common immersion pyrometer was not possible because of the small interior diameter of our crucible (38.1 mm). Despite the limitations associated with the lab-scale setup, the proposed synthesis method, when sufficiently developed, permits lab-scale trials of melting steel to produce steel syntactic foams [1]. A fifty percent reduction in weight and an increase in impact energy absorption make syntactic steel foam an attractive candidate for armor applications in military vehicles and improved crashworthiness in civilian vehicles, competitive with conventional solid steel alloys.

Please cite this article as Castro and S. Nutt , “**Synthesis of syntactic steel foam using mechanical pressure infiltration**” Mater Sci & Engrg A 535 (2012) 274-280 DOI<<http://dx.doi.org/10.1016/j.msea.2011.12.084>>



2. Experimental procedures

2.1 Materials

The materials selected to produce the syntactic steel foams were steel and hollow alumina microspheres (Washington Mills Company). Medium carbon steel with a target composition of 0.5% C and 1.4% Si was selected for initial trials. This composition was chosen because an increase in the level of silicon in steel reportedly increases melt fluidity by lowering the liquids temperature [3]. A low carbon steel with a composition of 0.2% C and 0.1% Si was also employed and tested. The composition of the alumina microspheres is shown in Table 1. The hollow microspheres (diameter ≈ 1.27 mm) were approximately spherical with a surface texture that was rough and irregular. Alumina microspheres were sorted and classified for the infiltration experiments. Additionally, microspheres that were broken or defective were separated from whole microspheres using a water buoyancy method. Typically, broken or defective spheres sank, while whole microspheres floated.

Table 1: Typical chemical analysis of alumina microballoons

Component	Percentage
Al ₂ O ₃ (by difference)	99.2
SiO ₂	0.60
Fe ₂ O ₃	0.02
Na ₂ O	0.15
CaO	0.01
Other oxides	0.02

Please cite this article as Castro and S. Nutt , “**Synthesis of syntactic steel foam using mechanical pressure infiltration**” Mater Sci & Engrg A 535 (2012) 274-280 DOI<<http://dx.doi.org/10.1016/j.msea.2011.12.084>>



2.2 Experimental procedures

The pressure infiltration procedure involved melting a prescribed quantity of steel in a free-standing crucible situated in a customized induction furnace (12.5 kW, 10–50 kHz). The steel melting capacity of the crucible was 580 g ($7.44 \times 10^{-5} \text{ m}^3$). Once the steel melted completely, alumina microspheres were added to the surface of the melt. Because of the high buoyancy and low wettability, microspheres floated on the melt surface. The graphite crucible (with the molten steel and microspheres) was then removed from the induction furnace and placed in an infiltration press. A mechanical infiltration press with a graphite plunger was applied to the microspheres, forcing the melt into the interstitial spaces between the packed microspheres (Fig. 1). Force was applied to overcome the inherent surface tension forces resisting infiltration. The resultant casting consisted of two regions: a dense layer of excess at the bottom, covered by a thick layer of syntactic steel foam. During the melting and infiltration process, the duration of each step was controlled to produce repeatable and consistent results. Several experiments were carried out to determine how process variables influenced the quality of the foam. Key variables included the temperature at which microspheres were preheated, the plunger travel distance, and the volume ratio of microspheres to steel. This will be discussed in more detail in Section 3.

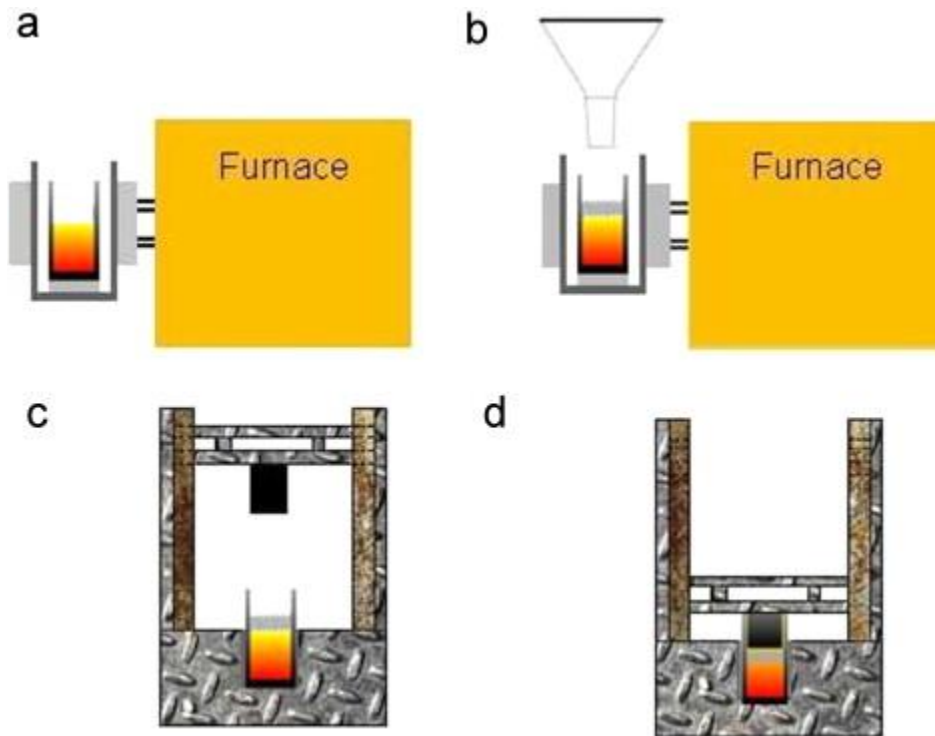


Figure 1: Infiltration process: (a) melting, (b) adding the microspheres, (c) initiation of the infiltration, and (d) infiltration finished.

2.3 Density calculation

Syntactic foam samples were sectioned to final dimensions of $\text{Ø } 33.8 \times 10 \text{ mm}$. The density of the syntactic foam was determined by measuring the weight and dimensions of the sample. Thus, the density of the steel syntactic foam sample was 4220 kg/m^3 , and the relative density of the syntactic foam sample was 0.54 (compared to solid steel – 7800 kg/m^3). Image analysis of polished sections revealed a microsphere volume fraction of 0.53. A random collection of spheres can be expected to yield a minimum packing density of 52.36% [7]. Therefore, a volume fraction of 0.53 corresponds roughly to random loose packing of microspheres. Usually, random dense packing occurs when a loose collection of spheres is vibrated to achieve greater packing efficiency [7].

Please cite this article as Castro and S. Nutt , “**Synthesis of syntactic steel foam using mechanical pressure infiltration**” Mater Sci & Engrg A 535 (2012) 274-280 DOI<<http://dx.doi.org/10.1016/j.msea.2011.12.084>>



2.4 Microstructure of the syntactic foam

Polished sections of cast foam samples were prepared to determine the distribution of microspheres and the quality of the infiltration. A typical distribution of microspheres in the steel matrix is shown in Fig. 2. Using a nearest neighbor analysis, an index value of 2 was determined, indicating that the distribution was “regular” – a value of 0 is characteristic of a clustered distribution, while a value of 2.15 indicates a regular distribution [8]. There was no evidence of microsphere clustering or unintended porosity (unfilled regions between the microspheres). Furthermore, there was no sign of broken or cracked microspheres that were infiltrated with steel in interior regions, indicating that total infiltration was obtained. Note that minor defects were occasionally observed. When two microspheres were nearly touching, molten steel did not flow around both microspheres completely, leaving a small gap at the point of contact.

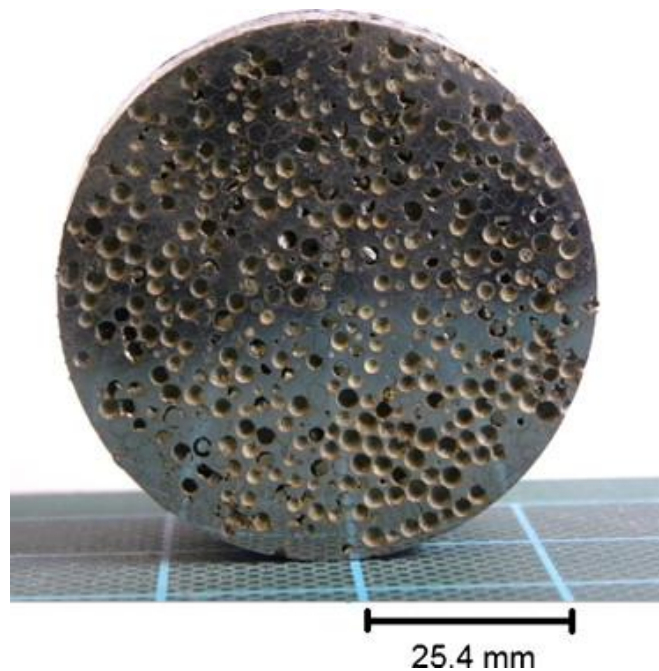


Figure 2: Medium carbon syntactic steel foam.

Polished and etched sections of the medium carbon steel syntactic foam revealed that the matrix consisted of two microconstituents: a large amount of a gray-colored phase (pearlite) and a small amount of a light-colored phase (pro-eutectoid ferrite). Ferrite is usually present in steel as a solid solution of iron containing carbon or one or more alloying elements such as silicon and manganese, while pearlite is present as a mixture of alternate strips of ferrite and cementite in a single grain. In contrast, sections of the low carbon steel syntactic foam revealed a large amount of ferrite and a small amount of pearlite (Fig. 3). At the top of Fig. 3a and b, there is an inset showing the region where the microstructure is observed.

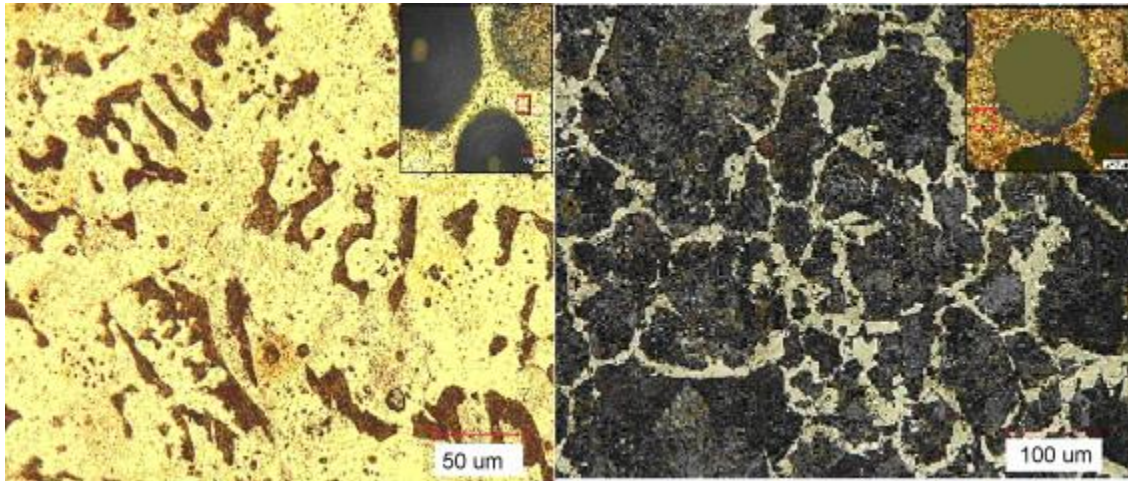


Figure 3: Microstructure of the low carbon steel syntactic foam (left). Microstructure of the medium carbon steel syntactic foam (right).

Hardness measurements were performed using a nanoindenter (Agilent – MTS XP) to determine the properties of the microconstituents of the carbon syntactic steel foams (ferrite and pearlite). The average hardness values of the microconstituents in the medium carbon steel syntactic foam sample were 2.55 GPa and 3.55 GPa for ferrite and pearlite, respectively. Each measurement was performed ten times at different locations of the sample. Comparing measured values with those reported in the literature, the values are in the same range for both phases. Mian reported a value of 2.43 GPa for AISI 1005 steel (predominantly ferrite) and 3.49 GPa for AISI 1045 steel (ferrite/pearlite) [9]. Material hardness is directly related to yield strength and resistance to plastic deformation [10]. Ferrite, the softer constituent, plastically deforms more readily than pearlite.

2.5 Compression

Compression tests of steel syntactic foam were conducted at a strain rate of 1 mm/min. The specimen dimensions were 8.38 mm × 8.38 mm × 11.68 mm. Four samples for each composition were

Please cite this article as Castro and S. Nutt , “**Synthesis of syntactic steel foam using mechanical pressure infiltration**” Mater Sci & Engrg A 535 (2012) 274-280 DOI<<http://dx.doi.org/10.1016/j.msea.2011.12.084>>



prepared by polishing prior to testing, and all foam samples tests had a relative density of 0.54. Load-displacement data were recorded during testing and subsequently converted to stress-strain data. The specimen size ensured that each sample tested contained at least six microspheres in each direction, thus minimizing edge effects [11].

3. Results and discussion

Production of syntactic steel foams using alumina microspheres presented challenges because of the poor wettability between the constituents and the high melt temperature of steel, which often caused rapid cooling and premature solidification. Another difficulty was the entrapment of air during melt infiltration. Key process variables for producing high quality foams were the preheating temperature of the microspheres, the travel of the plunger, and the ratio of microspheres/melt. The effects of these parameters are considered below.

3.1 Microsphere pre-heatment temperature

For complete infiltration of the microspheres, the melt must remain liquid during the entire process. Our infiltration experiments were non-isothermal, because the molten steel was always hotter than the preheated microspheres and the plunger. Thus, as the liquid steel flowed between the microspheres, some cooling invariably occurred. A completely isothermal infiltration process would eliminate the possibility of premature liquid steel solidification, but this is difficult to achieve in practice because of the high melting point of steel.

Please cite this article as Castro and S. Nutt , “**Synthesis of syntactic steel foam using mechanical pressure infiltration**” Mater Sci & Engrg A 535 (2012) 274-280 DOI<<http://dx.doi.org/10.1016/j.msea.2011.12.084>>



In initial experiments, microspheres were preheated in a resistance furnace to either 300 °C or 500 °C. However, the microspheres tended to cool rapidly once removed from the furnace and poured on the steel melt just prior to infiltration because of the low mass and high surface area of the microspheres. Similar difficulties were encountered during the infiltration of SiC preforms with cast iron [12]. The resulting samples showed incomplete infiltration associated with premature solidification of the melt.

Superior infiltration was achieved by adding microspheres directly to the melt surface in the induction furnace and holding for three minutes in the induction furnace to heat the microspheres. No attempt was made to measure the temperature of steel or the microspheres inside the induction furnace using an immersion or optical pyrometer because the liquid steel was covered by the alumina microspheres and a ceramic lid covered the crucible to avoid excessive heat losses and promote higher preheating temperature of the microspheres. The temperature of the microspheres prior to infiltration was undoubtedly higher using this technique than during initial trials. Increasing the time the microspheres were exposed to the heated melt increased the temperature of the microspheres (and of the melt, also), but three minutes was sufficient for equilibration, and extending the preheating time (more than three minutes) did not appear to benefit the infiltration process. The graphite plunger also was preheated to 600 °C to reduce the risk of premature solidification.

3.2 Plunger infiltration travel

Another challenge associated with pressure infiltration was air entrapment, which typically prevents complete infiltration of the syntactic foam. Multiple trials revealed that the rate of descent of the graphite plunger was critical to achieve infiltration without air pockets. The descent of the heated

Please cite this article as Castro and S. Nutt , “**Synthesis of syntactic steel foam using mechanical pressure infiltration**” Mater Sci & Engrg A 535 (2012) 274-280 DOI<<http://dx.doi.org/10.1016/j.msea.2011.12.084>>



plunger was thus achieved in two stages. In the first stage, the plunger was lowered to touch the microspheres in the crucible, allowing air to gradually escape from interstitial cavities as microsphere packing increased slightly. Melt infiltration during this stage was negligible, and some equilibration of plunger, microspheres, and melt occurred. In the second stage, a threshold stress of ~ 0.5 MPa was applied quickly to achieve melt infiltration of the microspheres. Interestingly, sub-threshold plunger stresses produced no infiltration, as the melt tended to “race-track” along crucible walls instead. Such experiments demonstrated the existence of this minimal stress required to achieve infiltration.

3.3 Amount of microspheres

The graphite crucibles provided a finite volume for the steel melt and the microspheres (0.0381 m interior diameter and 0.05 m height). Infiltration experiments were performed to determine the sample size and proportions of constituents to achieve complete infiltration. The following quantities of microspheres were employed: $6 \times 10^{-6} \text{ m}^3$, $12 \times 10^{-6} \text{ m}^3$, $18 \times 10^{-6} \text{ m}^3$ and $24 \times 10^{-6} \text{ m}^3$ (measured in a graduated tube). With $6 \times 10^{-6} \text{ m}^3$ and $12 \times 10^{-6} \text{ m}^3$, complete infiltration was achieved with minimal unintended porosity. However, when using $18 \times 10^{-6} \text{ m}^3$ and $24 \times 10^{-6} \text{ m}^3$, the quality of the resulting samples was poor, and foams contained substantial unintended porosity. The unintended porosity was attributed to premature solidification of the melt and associated inhibition of infiltration. While the melt volume was sufficient for infiltration, the thermal energy was insufficient to prevent premature freezing. We concluded that $12 \times 10^{-6} \text{ m}^3$ of microspheres was roughly the maximum volume of microspheres that could be used to produce a high-quality foam sample with our crucible size. Larger samples can be achieved using larger crucibles. It is interesting

Please cite this article as Castro and S. Nutt , “**Synthesis of syntactic steel foam using mechanical pressure infiltration**” Mater Sci & Engrg A 535 (2012) 274-280 DOI<<http://dx.doi.org/10.1016/j.msea.2011.12.084>>



to note that samples produced with $6 \times 10^{-6} \text{ m}^3$ and $12 \times 10^{-6} \text{ m}^3$ presented similar microsphere distribution and the same relative density (0.54). This is explained by the fact that the microspheres tended to float and aggregate at the top of the sample in the same pattern, producing similar microsphere distributions in those samples and subsequently equal relative density.

3.4 Interfacial reactions

Alumina and steel is a non-wetting system in which iron is the oxidizable phase. At high temperatures, interfacial reactions between alumina and steel are possible; including alumina dissolution in molten steel have been reported [13]. These reactions can affect interface structure and thus the mechanical behavior of syntactic steel foams [13]. The possible formation of an interface product requires diffusion, and thus the reaction depends strongly on the infiltration temperature and exposure time. Usually long exposure times (in the order of hours) and the high melting temperature of steel contribute to the development of the chemical reaction between liquid steel and alumina [14].

To determine if chemical dissolution of the alumina occurred, composition profiles were measured by X-ray spectroscopy (EDS) on polished syntactic foam sections. The probe was stepped across the interface between an alumina microsphere and the medium carbon steel, providing an opportunity to examine the region for evidence of interdiffusion and intercalation. Fig. 4 shows the microsphere-steel interface. Although the edge of the microsphere wall was not smooth, the border was clear and discrete. There was no visible interface layer between the microsphere and the steel matrix.

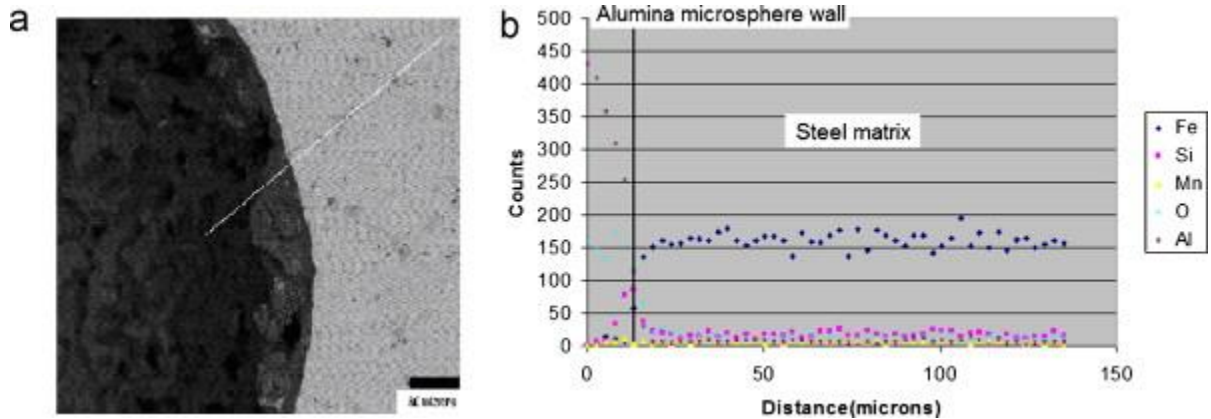


Figure 4: (a) The wall of an alumina microsphere observed in high magnification using back-scattered electron (BSE) imaging also indicating the line of scan. (b) EOS line scan at the interface between the steel and alumina microsphere.

The composition profile across the steel-alumina interface shows the distribution of elements in the region (Fig. 4). The Al and O content were constant within the microsphere wall (to the left of the line in Fig. 4b), then both decreased to almost zero in the steel matrix. Likewise, the Fe and Mn chemical contents were constant in the steel matrix (to the right of the line in Fig. 4(b)), then both decreased to almost zero at the microsphere wall. Therefore, there was no evidence that chemical reaction or diffusion between steel and alumina occurred at the interface. This could be explained by the fact that the time of contact between the molten steel and the alumina microspheres in our experiments were in the order of minutes. Because of the short solidification time, there was insufficient time for a dissolution reaction between the two phases.

3.5 Mechanical properties

Compared to conventional metallic foams, syntactic foams typically feature higher compression strengths, isotropic mechanical properties, and superior energy-absorbing capabilities due to extensive strain accumulation at relatively high stresses. The syntactic steel foam produced in this

Please cite this article as Castro and S. Nutt , “**Synthesis of syntactic steel foam using mechanical pressure infiltration**” Mater Sci & Engg A 535 (2012) 274-280 DOI<<http://dx.doi.org/10.1016/j.msea.2011.12.084>>



study exhibited a characteristic ductile stress–strain behavior when tested in compression (Fig. 5). The first stage was a linear elastic region, which was followed by a distinctive knee where the slope of the curve dropped to almost zero. The stress at this knee was taken as the compression strength for the foam. The knee was followed by a long stress plateau, during which the cell walls buckled and collapsed. Note that the slope in this region gradually increased as the deformation progressed and was not completely flat, as in an ideal energy absorber. The duration of the plateau depended on the relative density of the foam – normally foams with lower relative density present longer stress plateaus. The duration of the plateau region of our samples extended to approximately 50% strain, which is consistent with the relative density of our samples 0.54. Finally, the plateau ends and the stress began to rise sharply, as the microspheres were completely collapsed, and the densification stage began.

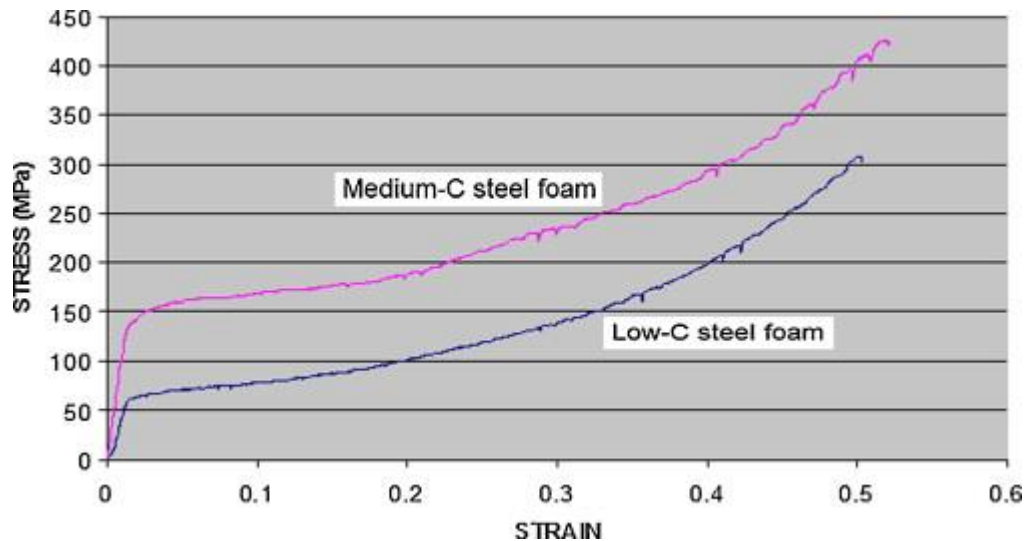


Figure 5: Stress–strain response of low carbon (bottom) and medium carbon (top) steel foam.

Please cite this article as Castro and S. Nutt , “**Synthesis of syntactic steel foam using mechanical pressure infiltration**” Mater Sci & Engrg A 535 (2012) 274-280 DOI<<http://dx.doi.org/10.1016/j.msea.2011.12.084>>



3.6 Compression strength

The compression strength of metal foams depends strongly on the relative density and the yield strength of the matrix material [15]. As the yield strength of the matrix increases, so does the compression strength of the resultant syntactic foam. This is apparent in the stress-strain curves of low carbon and medium carbon steel syntactic foams, shown in Fig. 5. The low-carbon steel foam exhibits a lower compression strength than the medium-carbon steel foam. Increasing the carbon content increases the yield strength of steel, and thus the foam. The low-carbon steel syntactic foam contained a largely ferritic microstructure which was not as strong as the pearlitic microstructure of the medium-carbon steel foam.

Insight into the mechanisms of deformation is provided by images of the foam sample recorded at progressively increasing strains, as shown in Fig. 6. The sample deformed smoothly throughout most of the compression range (up to 50% strain). Cell walls buckled continuously and collapsing cells were uniformly distributed through the sample during compression. After the cell collapse mechanism was exhausted, the ceramic microspheres were completely crushed, and some pulverized fragments exfoliated from the sample. Steel foams with high carbon content (2%–3% C: gray iron matrix) normally present serrated stress–strain curves, with large stress drops in the stress plateau [1]. This behavior is considered undesirable for the energy absorption function of metallic foams because the serrations are associated with cell wall cracking and fragmentation in a brittle manner, as opposed to plastic bending [1]. Fragmentation behavior has not been observed in any of the syntactic steel foams produced here – the foams remain intact and in one piece after compression loading.

Please cite this article as Castro and S. Nutt , “**Synthesis of syntactic steel foam using mechanical pressure infiltration**” Mater Sci & Engrg A 535 (2012) 274-280 DOI<<http://dx.doi.org/10.1016/j.msea.2011.12.084>>

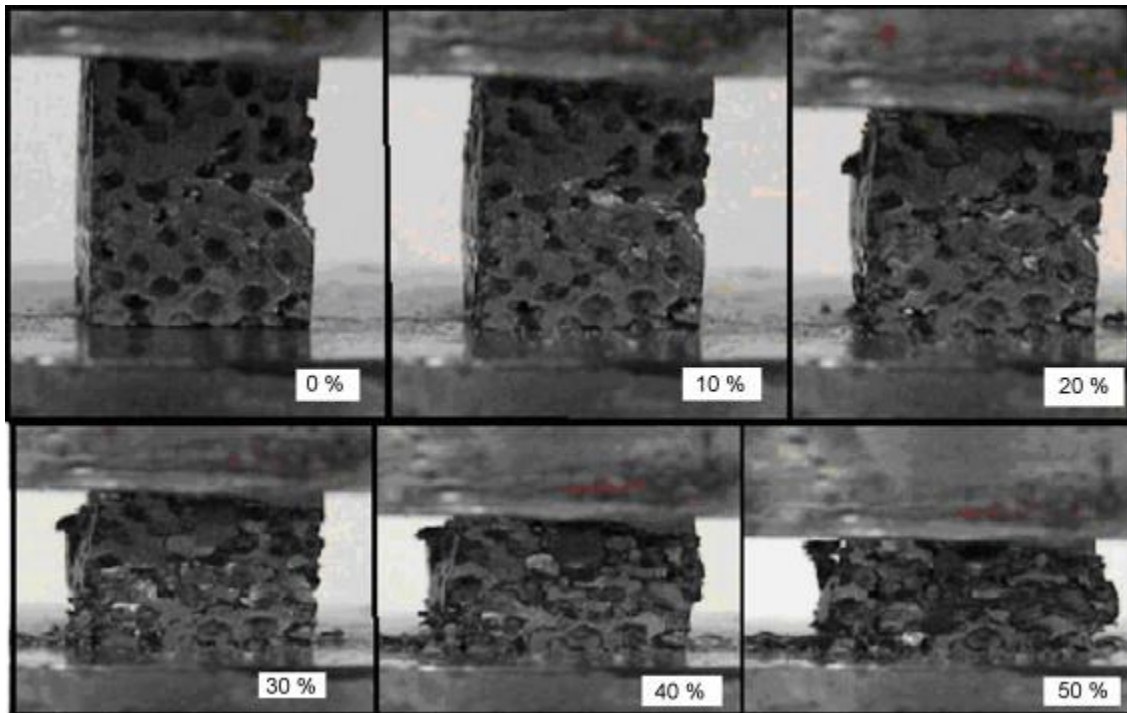


Figure 6: Compression of medium carbon syntactic steel foam: showing different stages of compression: 0%, 10%, 20%, 30%, 40% and 50% strain.

3.7 Energy absorption of steel syntactic foams

During compression of the syntactic steel foam, the work done is irreversibly absorbed as plastic deformation. The energy absorbed per unit volume is given by the area under the stress–strain curve up to the onset of densification. A common objective in producing metal foam is to maximize the amount of energy absorbed by increasing the height of the stress plateau (compression strength) as well as the duration of the stress plateau (densification strain).

The compression behavior of the steel syntactic foam produced here is compared with other steel foams in Table 2 (Fig. 7). The table includes properties for a stochastic steel foam produced by a powder metallurgical method [1], as well as properties for a composite syntactic foam produced by

Please cite this article as Castro and S. Nutt , “**Synthesis of syntactic steel foam using mechanical pressure infiltration**” Mater Sci & Engrg A 535 (2012) 274-280 DOI<<http://dx.doi.org/10.1016/j.msea.2011.12.084>>



filling the interstitial spaces between densely packed steel microspheres with steel powder and sintering them into a solid cellular structure [2]. Table 2 shows that the low-carbon syntactic steel foam exhibits an energy absorption capacity of 69.45 MJ/m^3 , while the medium-carbon syntactic steel foam has a value of 122.68 MJ/m^3 . The low-carbon steel foam thus has an energy absorption capacity comparable to the steel foam produced in references 2 and 3. On the other hand, the medium carbon steel foam shows greater energy absorption per unit volume and also greater energy absorption per unit mass than any of the other steel foams.

Please cite this article as Castro and S. Nutt , “**Synthesis of syntactic steel foam using mechanical pressure infiltration**” Mater Sci & Engrg A 535 (2012) 274-280 DOI<<http://dx.doi.org/10.1016/j.msea.2011.12.084>>



Table 2: Comparison of physical properties of our samples with other steel foams.

	Powder metallurgy carbon steel foam[2]	Powder metallurgy stainless steel foam[2]	Blowing agent steel foam high density [3]	Blowing agent steel foam low density [3]	Medium carbon syntactic metal foam	Low carbon syntactic metal foam
Sphere OD (mm)	1.4	2	*	*	1.27	1.27
Sphere wall thickness (mm)	0.05	0.1	*	*	0.04	0.04
Measured density (g/cm ³)	2.55	2.95	4.34	3.52	4.21	4.21
Relative density (%)	32.40	37.50	55.60	45.12	54.0	54.0
Densification strain (%)	57.00	54.00	50.00	50.00	50.00	50.00
Energy absorption per volume at densification (MJ/m ³)	37.60	67.80	85.00	50.00	122.68	69.45
Energy absorption per mass at densification (kJ/kg)	14.75	22.98	19.59	14.20	29.14	16.50

Please cite this article as Castro and S. Nutt , “**Synthesis of syntactic steel foam using mechanical pressure infiltration**” Mater Sci & Engrg A 535 (2012) 274-280 DOI<<http://dx.doi.org/10.1016/j.msea.2011.12.084>>

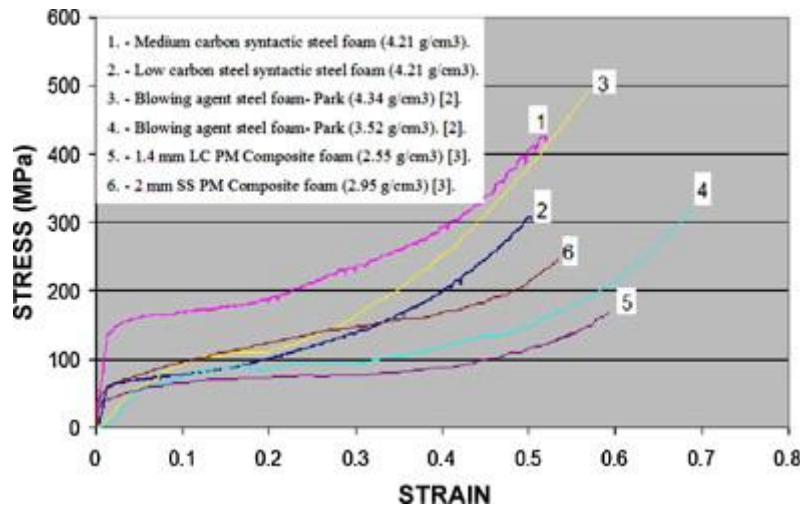


Figure 7: Stress–strain curves of our foams and steel foams from references 2 and 3.

The stochastic high density steel foam produced in reference 2 has one of the highest energy absorption capacities among all metal foams, 85 MJ/m^3 , but this value is significantly less than the medium-carbon steel foams produced in the present study (122 MJ/m^3). The stochastic foam of reference 2 is characterized by irregular, non-circular pores of different size [1]. In contrast, the composite syntactic foam described in reference 3 exhibits uniform pore sizes characteristic of syntactic foams. However, the high degree of matrix porosity may be responsible for the relatively low energy absorption capacity of these syntactic foams (67.80 MJ/m^3) [2]. In contrast, the foam described here presents a more uniform cell structure free of unintended porosity, largely because of the use of monosized microspheres and the absence of unintended porosity. Comparing the foam produced here with aluminum closed-cell foam [16] reveals that the aluminum foam absorbs 2.6 MJ/m^3 (6.5 kJ/kg) at 50% strain, a value much lower compared to the values reported for the present syntactic steel foams. Syntactic steel foams have much greater energy absorption values

Please cite this article as Castro and S. Nutt , “**Synthesis of syntactic steel foam using mechanical pressure infiltration**” Mater Sci & Engng A 535 (2012) 274-280 DOI<<http://dx.doi.org/10.1016/j.msea.2011.12.084>>



compared to traditional closed-cell aluminum foams (348% greater energy absorption per mass) and are well-suited to applications requiring high impact energy absorption.

The pressure infiltration method described here can be used to produce steel foams of various compositions with the addition of suitable alloying elements. This opens the possibility of increasing the energy absorption capacity of syntactic foams simply by selecting steel alloys with greater yield strength. For example, simply increasing the carbon content (to more than 0.5%) should further increase the foam strength, although at the expense of ductility, which could render the foams brittle and unsuitable for energy absorption purposes. Other options include the addition of small amounts of vanadium, niobium and/or titanium into low-carbon, medium-carbon or low-alloy steels with the purpose of increasing the strength of the steel (micro-alloyed steels) [17]. The use of more advanced alloys such as dual phase steel can be expected to yield high-strength steel foam [18]. We are presently exploring the use of austempered ductile iron, a high-strength, high ductility alloy produced by heat treatment of ductile iron [19].

Another approach to increase the energy absorption capacity of syntactic foam is to increase the volume fraction of microspheres by employing a bimodal distribution of microspheres (combining coarse and fine microspheres). This approach has been applied to aluminum syntactic foams [20], although as the plastic strain range increases (by reducing the relative density), the compression strength generally decreases. Therefore, there is a tradeoff and an optimum combination of relative density and strength that yields the maximum energy absorption. Additional decreases in the relative density beyond this will serve to decrease the energy absorption of the syntactic foam [20]. Efforts are currently devoted to improving the overall performance of the syntactic steel foams.

Please cite this article as Castro and S. Nutt , “**Synthesis of syntactic steel foam using mechanical pressure infiltration**” Mater Sci & Engrg A 535 (2012) 274-280 DOI<<http://dx.doi.org/10.1016/j.msea.2011.12.084>>



Most methods of producing the metal foams cannot be easily scaled up to mass production. Although it would be possible to produce larger samples, one challenge inherent in this method is that the steel foam samples are limited to simple geometries (a cylinder with a ratio of height/diameter equal to 0.3). The reason is the large temperature gradient between the liquid steel in the crucible and the graphite ram makes the liquid steel cool down fast as it travels in between the microspheres towards the ram, limiting the infiltration distance in the vertical direction. Another issue the mechanical pressure infiltration method described here is a batch process and is not suitable for high volume manufacture of metal foam.

4. Conclusions

The production of syntactic steel foams by pressure infiltration of hollow alumina microspheres with molten steel was demonstrated using two steel compositions. The relative density of the syntactic foams was 0.54 (corresponding to 4.3 g/m³) with monosized microspheres 1.27 mm in diameter.

There was no evidence of clustering, unintended porosity, or breakage of microspheres.

The most critical parameters in the manufacturing of the steel syntactic foams were the melt temperature, the preheat temperature of the microspheres prior to infiltration, the pressure infiltration schedule, and the ratio of microspheres to melt.

Syntactic steel foams produced in this study exhibited elastic-plastic foam behavior in compression – an initial linear elastic region was followed by a long stress plateau, and ultimately by densification. As expected, the compression strength and energy absorption was greater for the medium-carbon syntactic steel foam compared to the low-carbon syntactic steel foam. The syntactic

Please cite this article as Castro and S. Nutt , “**Synthesis of syntactic steel foam using mechanical pressure infiltration**” Mater Sci & Engrg A 535 (2012) 274-280 DOI<<http://dx.doi.org/10.1016/j.msea.2011.12.084>>



steel foams exhibited much greater strength and energy absorption capacity than steel foams reported previously, and are appealing candidate materials for future applications requiring impact energy absorption.

Acknowledgements: The authors are grateful to Mr. Roy Tsai and Mr. Ezra Pryor, for assistance with casting and infiltration experiments.

References:

1. C. Park, S.R. Nutt, *Mater. Sci. Eng. A* 288 (1) (2000) 111–118.
2. B.P. Neville, A. Rabiei, *Mater. Des.* 29 (2) (2008) 388–396.
3. B. Shah, K. Parsons, L. Swenson, *Mod. Cast.* 92 (2) (2002).
4. S.K. Hyun, H. Nakajima, *Mater Trans. (JIM)* 43 (3) (2002) 526–531.
5. K. Lemster, T. Graule, J. Kuebler, *Mater. Sci. Eng. A* 393 (1–2) (2005) 229–238.
6. K. Lemster, M. Delportea, T. Graulea, J. Kuebler, *Ceram. Inter.* 33 (7) (2007) 1179–1185.
7. A. Rabiei, A.T. O’Neill, *Mater. Sci. Eng. A* 404 (1–2) (2005) 159–164.
8. T.F. Cox, *Stat. Probab. Lett.* 1–4 (1) (1983) 161–170.
9. A.J.Mian, D. Nicholas, P.T.Mativenga, *Int.J.Adv.Manuf. Technol.* 50 (1–4)(2010) 163–174.
10. J.F. Shackelford, *Introduction of Material Science for Engineers*, 6th ed., 2005, pp. 220–221.
11. Y. Sirong, L. Jiaan, L. Yanru, L. Yaohui, *Mater. Sci. Eng. A* 457 (1–2) (2007) 325–328.
12. G. Standke, T. Müller, A. Neubrand, J. Weise, M. Göpfert, *Adv. Eng. Mater.* 12 (3) (2010) 189–190.
13. M. Bahrainia, T. Minghettib, M. Zoelligc, J. Schubertd, K. Berrothd, C. Schelleb, T. Graulea, J. Kuebler, *Compos. Part A* 40 (10) (2009) 1566–1572.
14. K. Nakashima, K. Takihira, K. Mori, N. Shinozaki, *Mater. Trans. (JIM)* 33 (10) (1992) 918–926.
15. L.J. Gibson, M.F. Ashby, *Cellular Solids Structure and Properties*, Cambridge University Press, 1999.
16. D. Ruan, G. Lu, F.L. Chen, E. Siores, *Compos. Struct.* 57 (1–4) (2002) 331–336.
17. A.A. Barani, F. Lia, P. Romanoa, D. Pongea, D. Raabea, *Mater. Sci. Eng. A* 463 (1–2) (2007) 138–146.
18. A. Gruttadauria, D. Mombelli, E.M. Castrodeza, C. Mapelli, *Matéria (Rio de Janeiro)* 15 (2) (2010) 192–198.
19. S.K. Putatunda, *Mater. Sci. Eng. A* 315 (1–2) (2001) 70–80.
20. X.F. Tao, L.P. Zhang, Y.Y. Zhao, *Mater. Des.* 30 (7) (2009) 2732–2736

Please cite this article as Castro and S. Nutt , “**Synthesis of syntactic steel foam using mechanical pressure infiltration**” *Mater Sci & Engrg A* 535 (2012) 274–280 DOI<<http://dx.doi.org/10.1016/j.msea.2011.12.084>>